

Kinematic Analysis of Robotic Arm Made with FRP Tubes for Material Transferring in Conveyors

Manchi Nageswara Rao¹, Arockia Selvakumar Arockia Doss²

Submitted: 12/05/2024 Revised: 25/06/2024 Accepted: 05/07/2024

Abstract: In order to avoid backlash disturbances, a conveyor control mechanism requires robotic path optimization with repeated cycle times. Using a magnetic gripper, this robotic manipulator moves raw steel materials from one conveyor to another. The present design uses a filament wound CFRP-Aluminum tube with 1.5mm thick layer. The actual arm deflection was analyzed with Taguchi DOE by selecting different parameters. Weights of 30 kg, 45 kg, and 60 kg were tested with 8,10,12 seconds of time for 100, 150, and 200 cycles with varying angular momentum. In terms of angular velocity, the span was 942.5mm, and the velocity was 8, 10, 12 mm/s, respectively. Our transient structural analysis used z-vector rotation as the rotation degree of freedom. Optimized parameters were compared against aluminium and GFRP wounded tube replacements using the 1DOF model. A 45kg load with 12 seconds of time and 7.88mm/s of travel time provided better results. CFRP shows a variation of 0.2mm in deformation after 150 cycles of rotation, while alumina shows a variation of 0.45mm and GFRP shows a variation of 0.8mm.

Keywords: Transient structural, Taguchi parameters, DOE, 1DOF, Kinematics, Deformation.

1. Introduction

Today, robotic arms are one of the most commonly used types of robotic systems. Robots can be classified according to their joints, degrees of freedom, and actuation mechanisms, among other things. Modern manipulators of industrial robots, as a rule, are made in the form of an open kinematic chain, in which each link has a separate electro-mechanical drive. Industrial robots have a certain number of degrees of freedom depending on the number of these drives. In various industries, robotic arms serve a variety of purposes with such technical solutions. [1]. It increases the weight of the robot arm and its dynamic loads when each kinematic link is driven by an electric or hydraulic motor. Using separate motors for each hand joint and finger of the gripper increases energy consumption. Various blanks, semi-finished products, and finished products can be held by the gripper of the robot arm [2]. This article proposes technical solutions for a robot arm and its gripper in the form of anthropomorphic structures, thereby increasing an industrial robot's technical capabilities, increasing its versatility due to the approximation to the functioning of a human hand and fingers [3]. With each finger having three movable links, this manipulator looks like a human hand and includes flexible kinematic links. There are a variety of shapes that can be grasped by this robot's

manipulator, such as rectangular, cylindrical, and spherical objects. However, all fingers of the gripper are driven by cables and act simultaneously, i.e., they cannot work independently[4]. Therefore, each phalanx of a finger cannot function offline. Using this design, it is possible to make a limited number of freeform products[5]. This robot's body is flexible due to elastic rods with deformable drives. Kinematic systems analyze the movement of bodies without taking force into account, and robot kinematics uses geometry to study the movement of multi-DOF kinematic chains that form robot manipulators. A joint parameter is specified, and a kinematic equation is used to calculate the end effector's position based on a specified value for each joint parameter. In forward kinematics, the robotic manipulator's position and orientation are calculated in terms of the joint variable. This current work is based on an industrial application with an 180^o-span area of selected area for a CFRP filament wounded aluminium tube.

2.0 Literature Review

In robotic kinematic analysis forward kinematic is simple to obtain but obtaining the inverse kinematics solution has been one of the main concerns in robot kinematics research. In this study to check technical solutions for a robot arm and its gripper in the form of anthropomorphic structures, which expand the technological capabilities of an industrial robot, increase its versatility due to the approximation to the functioning of a human hand and fingers of the gripper. One of the promising directions in the development of robotics is the creation of structures that are as close as possible to the skeleton and human

¹Research scholar ,School of Mechanical Engineering, Vellore Institute of Technology, Chennai - 600127, Tamil Nadu, India E- Mail address: nageswararao.manchi2017@vitstudent.ac.in

²Professor, School of Mechanical Engineering,Vellore Institute of Technology, Chennai - 600127, Tamil Nadu, India (correspondence) E-mail Address : arockia.selvakumar@vit.ac.in

image. This direction is explained by the desire to increase the versatility of industrial robots of classical design [6-7]. The well known robot manipulators are indefinite shape of bulk usage for example, agricultural products: vegetables and fruits pickings. In these cases, the classical designs of manipulators do not satisfy the production conditions. At present, original designs of gripping devices for robots are known, which are quite close to the device of a human hand. However, these devices operate on a rigid cycle and are not flexible enough for a variety of technological operations. For example, a soft robot arm [8-9] with tactile feedback for remote control is known. This hand is designed to perform complex tasks and ensure safe human-machine interaction. However, this hand works only with the direct participation of a person, more precisely the operator's hand, on which a glove with tactile sensors is put on to process information about the angles of the operator's hand joints. In general, inverse kinematics problems can be solved by using two type of approaches first one is closed form solutions and second is numerical approach. Closed form solutions are robot dependent and faster than the numerical approach. This approach classified into two type of methods Analytical method [10] and Geometric method [11]. Analytical method it is also called as algebraic method, analytically invert the direct kinematics equations. The problem of inverse kinematics can be summarized by solving a system of algebraic equations. Numerical approach method is not robot dependent so it can be applied to any kinematic arrangement, it is slower and, in some case, it is not possible to compute the solution. In this approach, there are different methods like symbolic elimination method [12], continuation method and iterative method. Symbolic elimination method eliminates variables from the set of non-linear equation to shorten it into a smaller set of equations. Different number of iterative methods are using now a day to resolve the inverse kinematics problems. However, this device does not have a gripping element for holding production objects. In works [13]-[15], original designs of anthropomorphic grips for manipulators are proposed, but these fingers of these grips work only in 2D space. Due to the indicated drawback, this device cannot work in the angular coordinate system of three-dimensional space. The problem of adapting the functions of an industrial robot [16] is not limited to the creation of anthropomorphic structures. The solution of this problem also requires the creation of an appropriate optimal control, the studies of which are presented in Prospective studies are projects to create robotic exoskeletons for the rehabilitation of the upper limb of a person [17] [18]. These works are examples of adaptation of the movement of a robot arm and a human hand. Pedipulators of a mobile robot [19] are made in the form of anthropomorphic structures, but this robot does not

contain devices for gripping and holding production objects. The surgical robot [20] has increased positioning accuracy due to a special program, but four degrees of freedom are not enough to simulate the movement of a human hand. The mobile robot [21] has three-tube soft drives, and uses vacuum suction cups as a gripper. The flexible body of this robot is as close as possible to the likeness of soft-bodied organisms. However, the vacuum grippers of this robot do not possess the in-variance that is characteristic [22] of the human hand. The above designs of anthropomorphic grippers indicate the prospects for their development, which confirms the relevance of this problem [23]. This research is focused on robot education with the help of simulation to give students more freedom to determine the robot movement so that the trial and error cycle can be avoided during the lesson. The simulation is developed for simple 2-DoF robot arm kinematics and can be used to simulate the movement of SCARA robot [24]. Inverse kinematic analysis which is done using Robo-Analyzer which has the ability to give optimum position and orientation of desired robotic arm, by considering the IKA, meta modeling is done to get an optimum design of arm using Solid works after that structural analysis of different designs are done using Ansys simulation tool, an optimum design of arm is recommended after evaluating the results [25]. In this study, kinematic and design analysis were performed of a four degrees of freedom robot arm with Denavit-Battenberg notation. This robot arm can be programmed for many purposes. For example, this purpose could be locating the right places of books in libraries.

The kinematic equations can be applied to a variety of dimensional motion problems that consider the motion of an object with constant acceleration. When problem-solving, the formula we choose should include the unknown variable, as well as three known variables.

Kinematic equation for circular motion are:

$$\omega = \omega_o + at \dots\dots\dots (1)$$

This kinematic equation shows a relationship between final velocity, initial velocity, constant acceleration, and time. We will explore this equation as it relates to physical robotic problems. This equation is set up to solve for velocity, but it can be rearranged to solve for any of the values it contains.

$$\theta = \omega_o t + \frac{1}{2}at^2 \dots\dots\dots (2)$$

$$\omega^2 = w_o^2 + 2a\theta \dots\dots\dots (3)$$

$$\theta = \frac{(\omega_o + \omega)}{2} t \dots\dots\dots (4)$$

This one relates an object's displacement to its average velocity and time. The right-hand side shows the final velocity plus the initial velocity divided by two – the sum

of some values divided by the number of values, or the average.

2.1 Significance of proposed work

Kinematic analysis is crucial in robotic applications as it helps in understanding the motion of the robotic arm without considering the forces causing the motion. This allows for precise control and optimization of the arm's movements, ensuring efficient and accurate material transferring. By analyzing the kinematics with FRP composites in consideration can design robotic systems that operate smoothly and meet the desired performance criteria. The present research proposes a base pay load up to 60 Kg as checked with conveyor designed weight of rolling condition maximum with affective motor torque. Composite FRP tubes offer several advantages, including high strength-to-weight ratio, corrosion resistance, and durability. These characteristics enhance the robotic arm's efficiency by reducing the overall weight, which allows for faster and more precise movements. Additionally, the corrosion resistance ensures longevity and minimal maintenance, thereby reducing downtime.

3. Methodology

The transient structural analysis of the selected conveyor robotic arm was performed at different velocities. This was done to check for repeatability variance in the

deformed arm after the load is removed. Two conveyors on the shop floor are used to shift steel materials, and an arm attached to a magnetic gripper with a pay weight of 8kg is considered. In the shop floor, the maximum bar weight is set at 50 kg, while the distance between conveyor centers is set at 0.5 meters. A standard height of 0.6 meters was taken for the base height, and the robot moved circularly with a span of 0.6 meters. In order to create the structural body, we used structural steel SS316 as the base column material at fixed end and composite CFRP-AL wound arms attached to the base. Design parameters were tested on Ansys work bench in kinematic circular motion to check repeatable strain on the base surface attached to the arm. Bush-based threaded attachments are used to prevent vibration and moment locking. The properties and the fits clearance are assumed to be null in the simulation. In this simulation, the load capacity included with gripper weight along with levels, time, and weight are integrated with L9 DOE to optimize the fixed weight for the selected arms. The kinematic analysis process involves determining the motion of the robotic arm without considering the forces that cause the motion. It includes calculating the position, velocity, and acceleration of different segments of the arm. By employing mathematical models and simulations, the movement and trajectory of the arm can be optimized for efficient material transfer.

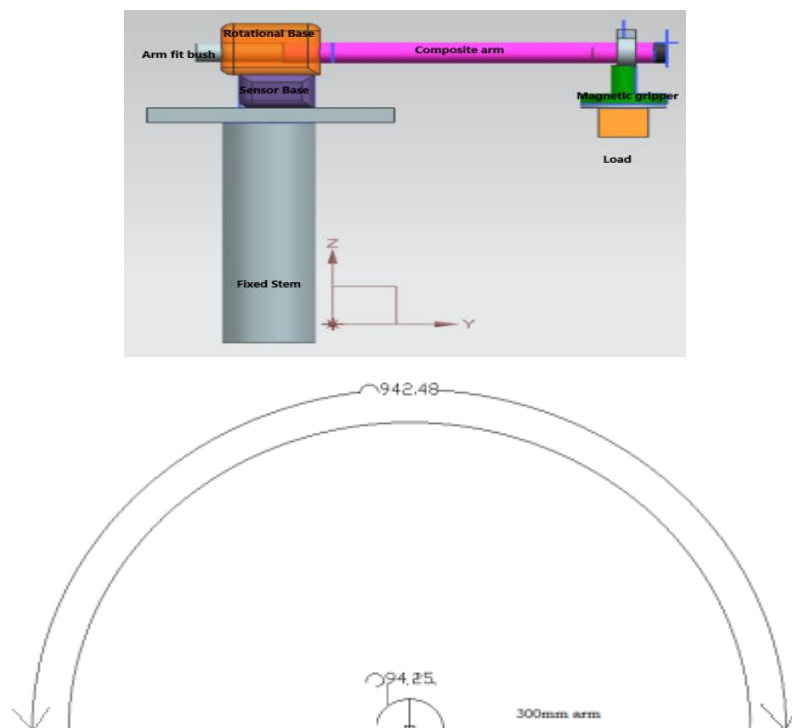


Fig 1: A) Designed model for Simulation B) Arm rotational span between two conveyors

The rotational distance taken as 94.25 mm for the axial pole the angular velocity divided as 3.14 radians of span for 180° levels are increased. According to travel time the

angular velocity(ω) fixed as 0.4rad/s,0.32 rad/s and 0.26rad/s respectively.

Table 1: Factors and levels for Taguchi DOE

Parameters	Level-1	Level-2	Level-3
Weight(Kg)	30	45	60
Travel Time(s)	8	10	12
Repeated cycles	100	150	200

In robotic applications, rigid body dynamics play an important role in determining the load carrying capacity of manipulator arms. As shown in figures 1 and 2, two

rotations of X and Y are fixed for the one degree of freedom with rotation along Z- vector with repeated cycles.

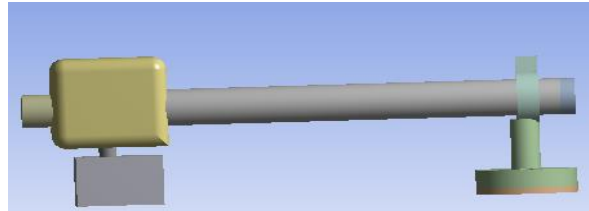


Fig :2 Revolute joint with body

Table 2 - Material properties

Property	CFRP-FW tube	Aluminium (6061)	GFRP-FW Tube
Tensile-UTS (Mpa)	74.63	290	59.1
Hardness (HV)	118.2	73.87	80.4
Modulus of Elasticity(GPa)	90.9	68.9	76.4
Thermal creep	0.02	0.01	0.03
Shear strength (MPa)	280	270	230
Fracture toughness MPa/m ²	32	29	28
Yield strength (MPa)	252	241	228

As shown in figures 3 and 4 with mesh condition in figure 3b, the arm fixed with rotation material assignment for the arm tube changed as per above experiments for CFRP and final optimal load conditions compared with AL and GFRP-FW tubes.

3.1 Importance of various load checking

Load applicability refers to the ability of the robotic arm to handle and transfer various weights and types of materials efficiently. It involves assessing whether the arm can maintain its performance and stability under different load conditions. This is crucial for ensuring that the

robotic arm can operate effectively in a conveyor system without failure or reduced accuracy.

The load range of 30kg to 60kg is significant because it represents typical operational stresses that the composite FRP arm might encounter in practical applications. This range allows for a comprehensive understanding of the material's performance under realistic conditions. The findings indicate how well the arm can withstand varying degrees of stress, ensuring reliability and safety in its intended use.

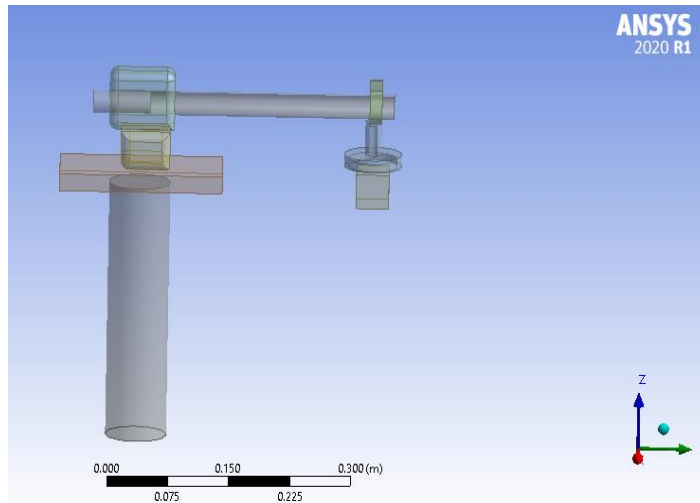


Fig:3a) Ansys Import model

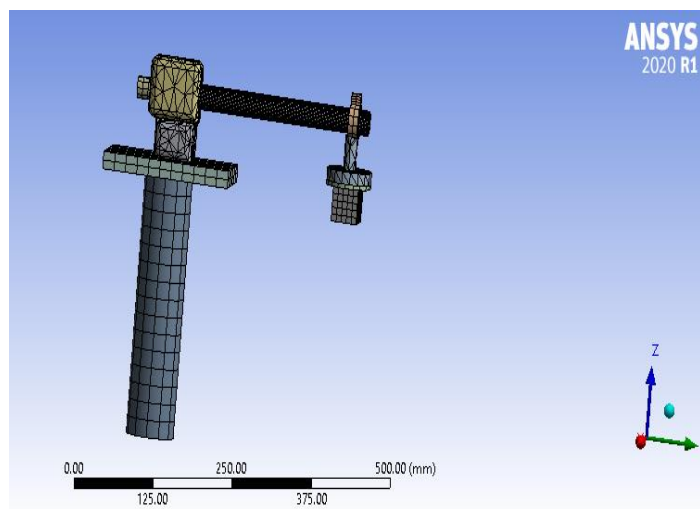


Fig: 3b) 3D model mesh for dynamic analysis

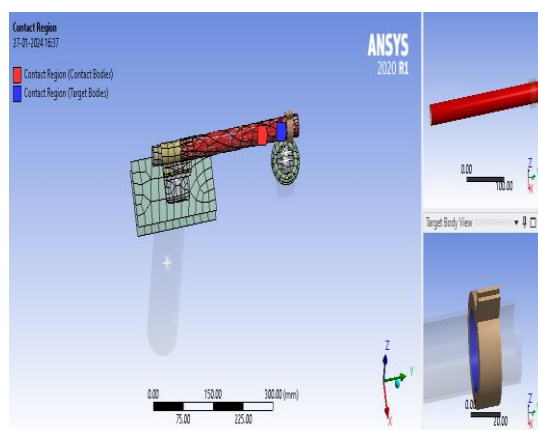


Fig 4: Material assignment with CFRP hybrid material assignment.

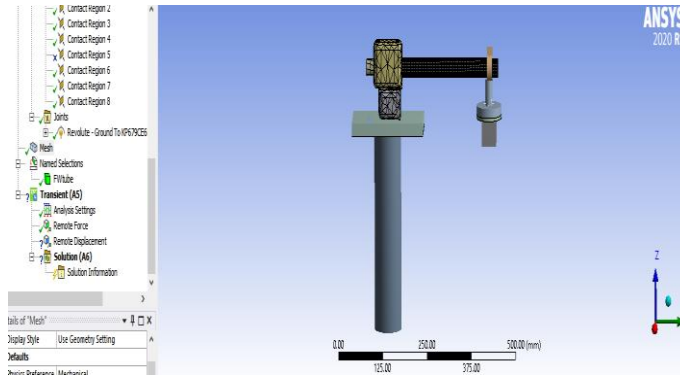


Fig 5: Load assignment CFRP tube

Figures 5 and 6 show revolute joints with body material assignments other than the tube. The materials are stainless steel for the base joint and the magnetic gripper

at the end of the arm for fixed conditions, and the block assigned for variable load conditions.

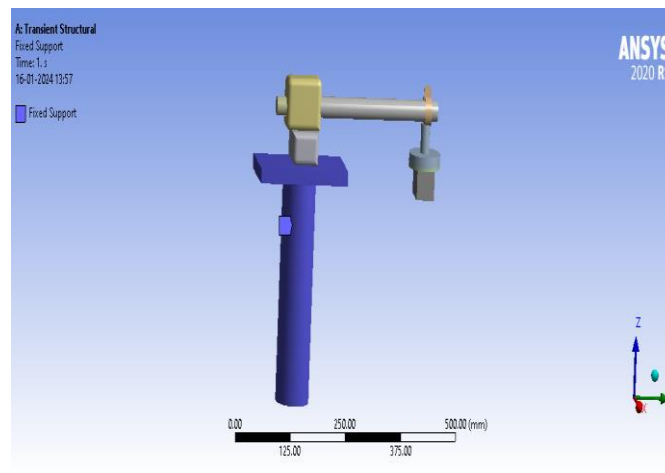


Fig 6: a) Fixed support

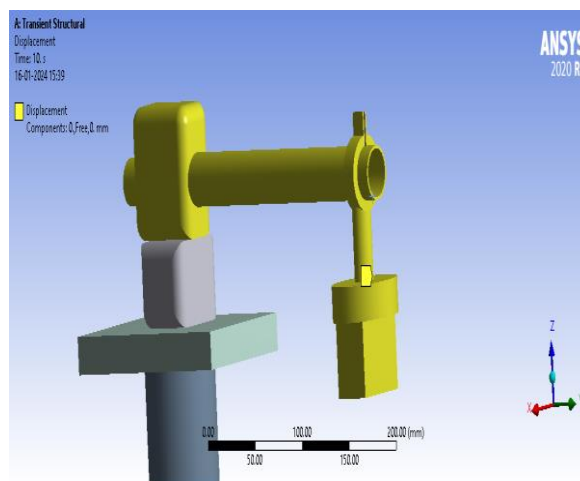


Fig 6: b) Rotating body with re-volute joint

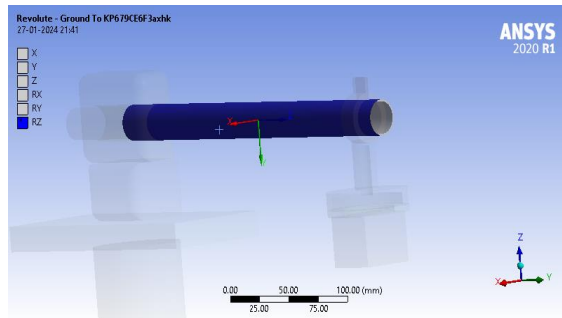


Fig 7: Deformation body selection with rotational Z- vector

According to figure7, the assumed FW CFRP tube is rotated along the principle vector, and the deformed directions are assigned along Z for checking the total deformation in the tube for repeatable cycles.

Results from the analysis shown for CFRP tube including payload for 60Kg to check the viability of the tube as shown in figure 8, with loading condition the maximum deformed bend is 1.5mm which shown in revolution section.

4.0 Results and discussions

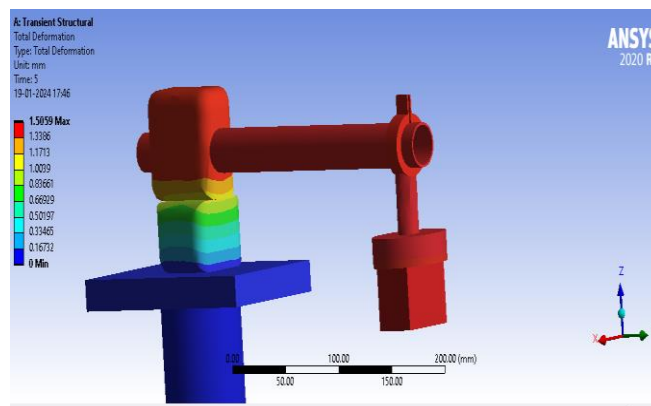


Fig 8: Total Deformation

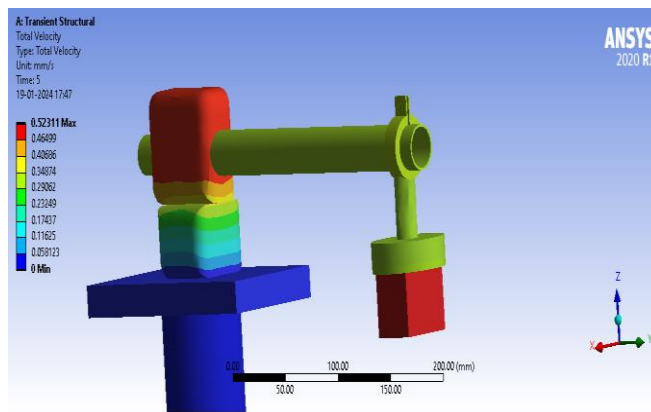


Fig 9: Total velocity

Considering the load block and revolution block as a single unit, the total affective velocity difference in the load block and revolution joint end would be 0.3mm/s - 0.52mm/s. As shown in figure 9, the impact velocity difference in the revolution joint end would be 0.52mm/s

- 0.3mm/s. The revolution pin attachment area and the tube fit area show a total elastic strain of 0.022 mm, while the tube and magnet areas do not show any real strain as shown in Figure 10.

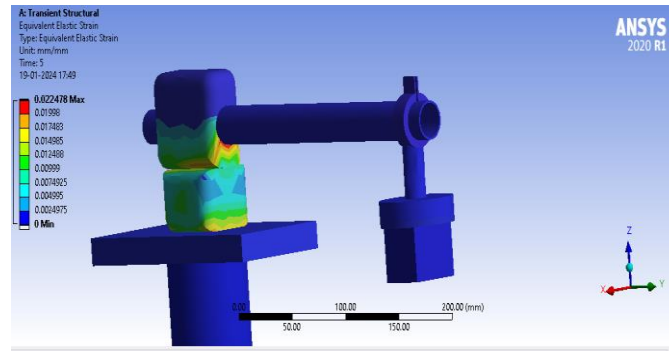


Fig 10: Elastic Strain

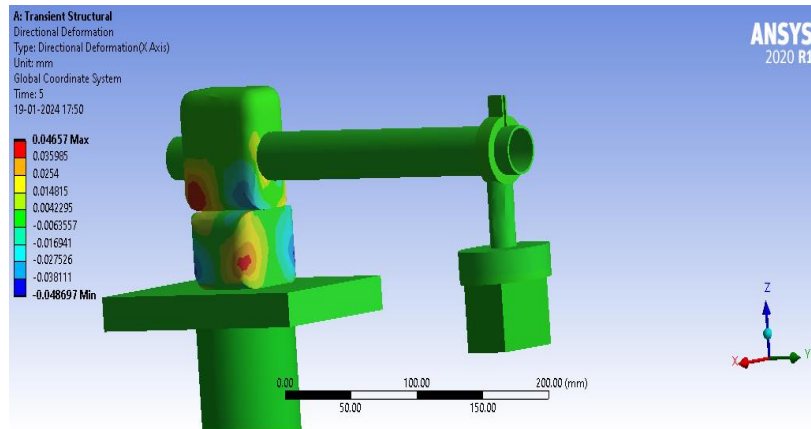


Fig 11: Directional deformation

In the selected span, the revolutionary body had a rotational deformation of 0.14mm at the tube-to-rigid body interface (figure 11).
directional deformation of 0.0042mm, with a maximum

Table 3: Results for orthogonal array in simulation

S.NO	Weight (kg) P-1	Time (sec) P-2	R-cy (P-3)	Total deformation (mm)	Variable velocity (mm/s)	Total deflection (mm/unit)
1	30	8	100	0.42	0.15	0.0042
2	30	10	150	0.39	0.12	0.0039
3	30	12	200	0.36	0.16	0.0048
4	45	8	150	0.72	0.27	0.0078
5	45	10	200	0.66	0.23	0.0091
6	45	12	100	0.6	0.18	0.0072
7	60	8	200	1.5	0.29	0.0224
8	60	10	100	1.2	0.27	0.0152
9	60	12	150	1.32	0.23	0.0136

4.1 Taguchi optimal analysis for CFRP tube

Taguchi optimization for DOE -L9 array considered for minimizing number of analysis in a mathematical approach using Mini-Tab.

Table: 4 Analysis of Variance for Means

Source	DF	Seq SS	Adj SS	Adj MS	F	P
A	2	0.369154	0.369154	0.184577	189.73	0.005
B	2	0.008159	0.008159	0.004080	4.19	0.193
C	2	0.004158	0.004158	0.002079	2.14	0.319
Residual Error	2	0.001946	0.001946	0.000973		
Total	8	0.383417				

Table 5: Response for Signal to Noise Ratios and means: Smaller is better

Level	S/N Ratio			Means		
	A	B	C	A	B	C
1	11.2056	5.2985	6.4725	0.1972	0.4457	0.3744
2	6.6428	6.4110	5.8834	0.3340	0.3797	0.4092
3	0.5039	6.6428	5.9965	0.6785	0.3843	0.4261
Delta	10.7017	1.3443	0.5891	0.4814	0.0660	0.0516
Rank	1	2	3	1	2	3

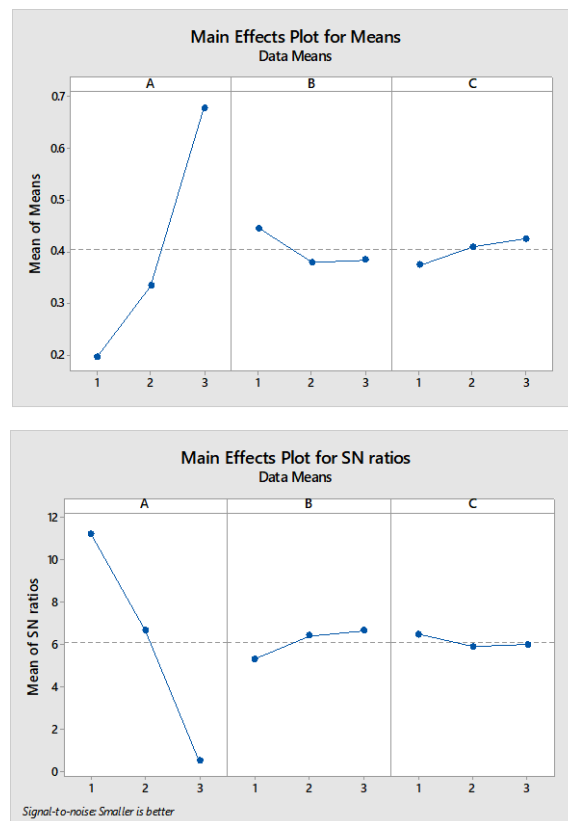


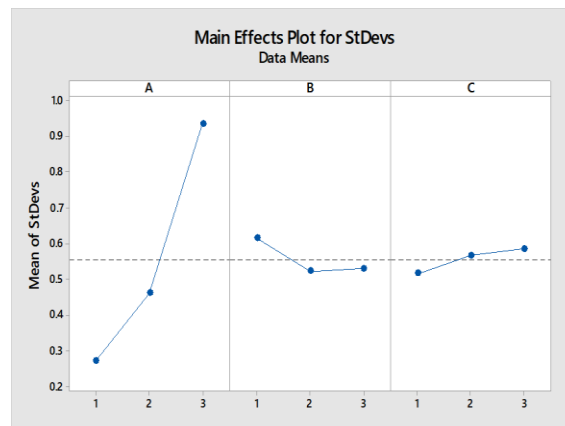
Figure 12: Parameter responses for mean and S/N ratio

The deviation observed in figure 12 is mainly between 45 to 60 kg, and the other two parameters, time and number of repeated cycles, are gradually different. There was no

significant change in factor 3 number of cycles between 150 and 200, meaning that the deformation is mainly determined by the block's weight and travel time.

Table 6: Estimated Model Coefficients for Standard Deviation

Term	Coef	SE Coef	T	P
Constant	0.55640	0.01398	39.803	0.001
A 1	-0.28367	0.01977	-14.349	0.005
A 2	-0.09539	0.01977	-4.825	0.040
B 1	0.05775	0.01977	2.921	0.100
B 2	-0.03272	0.01977	-1.655	0.240
C 1	-0.03941	0.01977	-1.994	0.184
C 2	0.01039	0.01977	0.526	0.652



Model Summary for the analysis of alpha 0.0419(s) the adjustable mean is 98.6% accurate in analyzing the data with R-sq mean of 99.52%

Table: 7 Analysis of Variance for Standard Deviation and Response

Source	DF	Seq SS	Adj SS	Adj MS	F	Level	A	B	C
A	2	0.699750	0.699750	0.349875	198.95	1	0.2727	0.6141	0.5170
B	2	0.015095	0.015095	0.007547	4.29	2	0.4610	0.5237	0.5668
C	2	0.007509	0.007509	0.003755	2.13	3	0.9355	0.5314	0.5854
Residual Error	2	0.003517	0.003517	0.001759		Delta	0.6627	0.0905	0.0684
Total	8	0.725871				Rank	1	2	3

Table: 8 Taguchi prediction (ANOVA) with ranking

S.NO	P-1	P-2	P-3	S/N Ratio	Mean	StDev	Ln(StDev)	Rank
1	30	8	100	10.7417	0.21085	0.291069	-1.24742	4
2	30	10	150	11.2651	0.1796	0.250410	-1.30671	5
3	30	12	200	11.6101	0.201	0.276714	-1.34987	3
4	45	8	150	5.58974	0.3825	0.529152	-0.654194	8
5	45	10	200	6.81545	0.3333	0.457310	-0.799271	2
6	45	12	100	7.52320	0.28625	0.396569	-0.877949	1
7	60	8	200	0.435941	0.74385	1.02222	-0.353682	7
8	60	10	100	0.795211	0.66555	0.920818	-0.102597	6
9	60	12	150	1.15258	0.6262	0.863330	-0.145224	9

The Taguchi prediction for the selected experiments was taken into consideration for the optimal parameter selection, resulting in 45kg load and 10 seconds run time

in the CFRP tube model, and 150 or 200 runs feasible. Based on the model run with the optimal parameters and 3 materials, the following results were obtained.

Table 9: Comparative table for different material arms

Arm component	Total deformation (mm)	Variable velocity (mm/s)	Total deflection (mm/unit)
CFRP -FW TUBE	1.42	0.17	0.0038
AL- TUBE	1.56	0.19	0.0052
GFRP- FW TUBE	1.72	0.24	0.0098

5. Conclusions

A conveyor system has been designed with a pick and place robotic manipulator to transport ferrous blocks. An arm made from CFRP filament wounded aluminium tube is equipped with a magnetic gripper. Experiments done using ANSYS workbench simulator for the optimal deviation from the deformed tube used as an arm. Rigid dynamics module simulated for selected manipulator model with a revolute connection between arm and base. An axis with a Z-vector can only be considered at a span of 180 degrees and a radius of 300mm. Weight and travel time were optimized with variable speeds, repeated cycles, and compared to aluminium arm and GFRP-wounded tube. Kinematic analysis with 100,150 and 200 fixed repeated cycles with Z. vector selected for rotation with variable carrying loads, structural variations are observed. Based on the results of the L9-experimentation, after 200 runs of maximum cycles for the different load conditions, it was determined that the maximum deformation was 0.022mm after removing the load. CFRP tube was found to provide better results compared with others. The findings suggest that the composite FRP arm exhibits excellent resilience under varying load conditions, indicating potential for enhanced durability in future designs. Designers can leverage this data to optimize material selection and structural configurations. This could lead to more efficient, lightweight, and robust components in engineering applications. The durability of composite FRP tubes also means the arm can handle heavy loads and operate in harsh environments without compromising performance. These properties make them ideal for use in robotic arms that require precise and reliable performance. Additionally, their lightweight nature helps to reduce the overall energy consumption of the system, enhancing efficiency.

References

- [1] P. Mesmer, M. Neubauer, A. Lechler, and A. Verl, "Robust design of independent joint control of industrial robots with secondary encoders," *Robotics and Computer-Integrated Manufacturing*, vol. 73, p. 102232, Feb. 2022, doi: 10.1016/j.rcim.2021.102232.
- [2] W. S. Pambudi, E. Alfianto, A. Rachman, and D. P. Hapsari, "Simulation design of trajectory planning robot manipulator," *Bulletin of Electrical Engineering and Informatics*, vol. 8, no. 1, pp. 196-205, Mar. 2019, doi: 10.11591/eei.v8i1.1179.
- [3] M. Li et al., "Design and performance characterization of a soft robot hand with fingertip haptic feedback for teleoperation," *Advanced Robotics*, vol. 34, no. 23, pp. 1491-1505, Dec. 2020, doi: 10.1080/01691864.2020.1822913.
- [4] Sharma and M. M. Noel, "Design of a low-cost five-finger anthropomorphic robotic arm with nine degrees of freedom," *Robotics and Computer-Integrated Manufacturing*, vol. 28, no. 4, pp. 551-558, Aug. 2012, doi: 10.1016/j.rcim.2012.01.001.
- [5] P. Dubey, S. M. Pattnaik, A. Banerjee, R. Sarkar, and S. K. R., "Autonomous Control and Implementation of Coconut Tree Climbing and Harvesting Robot," *Procedia Computer Science*, vol. 85, pp. 755-766, 2016, doi: 10.1016/j.procs.2016.05.263.
- [6] M. Li et al., "Design and performance characterization of a soft robot hand with fingertip haptic feedback for teleoperation," *Advanced Robotics*, vol. 34, no. 23, pp. 1491-1505, Dec. 2020, doi: 10.1080/01691864.2020.1822913.
- [7] A. Sipos and P. L. Várkonyi, "The longest soft robotic arm," *International Journal of Non-Linear Mechanics*, vol. 119, p. 103354, Mar. 2020, doi: 10.1016/j.ijnonlinmec.2019.103354.
- [8] F. Xu, H. Wang, J. Wang, K. W. S. Au, and W. Chen, "Underwater Dynamic Visual Servoing for a Soft Robot Arm with Online Distortion Correction," *IEEE/ASME Transactions on Mechatronics*, vol. 24, no. 3, pp. 979-989, Jun. 2019, doi: 10.1109/TMECH.2019.2908242.
- [9] J. Narayan, S. Mishra, G. Jaiswal, and S. K. Dwivedy, "Novel design and kinematic analysis of a 5-DOFs robotic arm with threefingered gripper for

- physical therapy,” *Materials Today: Proceedings*, vol. 28, pp. 2121-2132, 2020, doi: 10.1016/j.matpr.2020.04.017
- [10] E. Oyama, N. Y. Chong, A. Agah, T. Maeda, and S. Tachi, (2001) Inverse kinematics learning by modular architecture neural networks with performance prediction networks, in *Proc. IEEE International Conference on Robotics and Automation*, Pp.1009-1012.
- [11] Ramdane-Cherif, B. Daachi, A. Benallegue, and N. Levy, (2002) Kinematic inversion, in *Proc. IEEE/RSJ International Conference on Intelligent Robots and Systems*, 1904- 1909.
- [12] Nalin Raut, Abhilasha Rathod and Vipul Ruiwale. Forward Kinematic Analysis of a Robotic Manipulator with Triangular Prism Structured Links. *International Journal of Mechanical Engineering and Technology*, 8(2), 2017, pp. 08–15.
- [13] Ahuactzin J. M., Gupta K. K., "The kinematic roadmap: a motion planning based global approach for inverse kinematics of redundant robots", *IEEE Transactions on Robotics and Automation*, vol. 15(4), 1999, pp. 653-669.
- [14] S. Sarvarov, V. F. Mikhaylets, A. E. Vasilev, and K. V. Danilenko, “Analytical study of underactuated mechanisms of anthropomorphic robotic gripper,” in 2017 International Conference on Industrial Engineering, Applications and Manufacturing (ICIEAM), May 2017, pp. 1-5, doi: 10.1109/ICIEAM.2017.8076204.
- [15] H. Heidari, M. J. Pouria, S. Sharifi, and M. Karami, “Design and fabrication of robotic gripper for grasping in minimizing contact force,” *Advances in Space Research*, vol. 61, no. 5, pp. 1359-1370, Mar. 2018, doi: 10.1016/j.asr.2017.12.024.
- [16] K. Xu, Z. Liu, B. Zhao, H. Liu, and X. Zhu, “Composed continuum mechanism for compliant mechanical postural synergy: An anthropomorphic hand design example,” *Mechanism and Machine Theory*, vol. 132, pp. 108-122, Feb. 2019, doi: 10.1016/j.mechmachtheory.2018.08.015
- [17] M. A. Muslim, M. Rusli, A. R. Zufaryansyah, and B. S. K. K. Ibrahim, “Development of a quadruped mobile robot and its movement system using geometric-based inverse kinematics,” *Bulletin of Electrical Engineering and Informatics*, vol. 8, no. 4, December 2019, doi: 10.11591/eei.v8i4.1623.
- [18] Parkhomey, J. Boiko, and O. Eromenko, “Identification information sensors of robot systems,” *Indonesian Journal of Electrical Engineering and Computer Science*, vol. 14, no. 3, p. 1235, Jun. 2019, doi: 10.11591/ijeecs.v14.i3.pp1235-1243.
- [19] Gupta, A. Singh, V. Verma, A. K. Mondal, and M. K. Gupta, “Developments and clinical evaluations of robotic exoskeleton technology for human upper-limb rehabilitation,” *Advanced Robotics*, vol. 34, no. 15, pp. 1023-1040, Aug. 2020, doi: 10.1080/01691864.2020.1749926.
- [20] V. Yaglinsky, A. Al-Obaydi, G. Kozeratsky, and N. Moskvichev, “Kinematics Rods of Simulator-Hexapod,” *British Journal of Applied Science & Technology*, vol. 16, no. 3, pp. 1-7, Jan. 2016, doi: 10.9734/BJAST/2016/26274.
- [21] Kanada, F. Giardina, T. Howison, T. Mashimo, and F. Iida, “Reachability Improvement of a Climbing Robot Based on Large Deformations Induced by Tri-Tube Soft Actuators,” *Soft Robotics*, vol. 6, no. 4, pp. 483-494, Aug. 2019, doi: 10.1089/soro.2018.0115
- [22] Parkhomey, J. Boiko, N. Tsopa, I. Zeniv, and O. Eromenko, “Assessment of quality indicators of the automatic control system influence of accident interference,” *TELKOMNIKA (Telecommunication Computing Electronics and Control)*, vol. 18, no. 4, p. 2070, Aug. 2020
- [23] Arif Widodo Ahsan Muzakki, Farid Baskoro, A 2-DoF Robot Arm Simulation for Kinematics Learning, 2nd International Conference on Vocational Education and Training (ICOVET 2018), *Advances in Social Science, Education and Humanities Research*, volume 242.
- [24] Kazim Raza a , Tauseef Aized Khan b , Naseem Abbas, Kinematic analysis and geometrical improvement of an industrial robotic arm, *Journal of King Saud University – Engineering Sciences* 30 (2018) 218–223
- [25] Yasar, S. A., Korkut, I, Design and Kinematic Analysis Of A RRPR Robot Arm, *International Journal of Innovative Research in Engineering & Management (IJIREM) ISSN: 2350-0557, Volume-3, Issue-6, November-2016.*
- [26] Selvakumar.A. Arockia, “A numerical approach for 3 PRS Parallel manipulator”, *International Journal of Engineering & Technology*, Vol.7 No.4(2018): PP: 90-94.
- [27] Rishabh Jain, Mohd. Nayab Zafar , J. C. Mohanta, “Modeling and Analysis of Articulated Robotic Arm for Material Handling Applications” *Materials Science and Engineering* 691 (2019) 012010 IOP Publishing doi:10.1088/1757-899X/691/1/012010.
- [28] Arif Şirinterlikçi, Murat Tiryakioğlu*, Adam Bird, Amie Harris, Kevin Kweder, “Repeatability and Accuracy of an Industrial Robot: Laboratory Experience for a Design of Experiments Course” *the Technology Interface Journal/Spring 2009.*